Optics and Laser Technology 129 (2020) 106296

Contents lists available at ScienceDirect

Optics and Laser Technology

journal homepage: www.elsevier.com/locate/optlastec

Microfiber Fabry-Perot interferometer used as a temperature sensor and an optical modulator

Jin Li[a,b,*], Zhoubing Li[a], Juntong Yang[a], Yue Zhang[a], Chunqiao Ren[a]

[a] College of Information Science and Engineering, Northeastern University, Shenyang 110819, China

[b] State Key Laboratory of Applied Optics, Changchun Institute of Optics, Fine Mechanics and Physics, Chinese Academy of Sciences, Changchun 130033, China

HIGHLIGHTS

- A capillary encapsulated miniature temperature probe was proposed.
- The Fabry-Perot is composited by microfiber taper and single mode fiber.
- Temperature sensitivity of 6.386 nm/°C was experimentally demonstrated.
- Potential optical modulation phenomenon was observed.

ARTICLE INFO

Keywords:
Microfiber sensor
Temperature sensor
Integrated optics
Fiber optics

ABSTRACT

In this paper, a microfiber Fabry-Perot interferometer temperature probe is proposed by fixing and encapsulating a microfiber and single-mode fiber in the silica capillary using polydimethylsiloxane (PDMS). In this structure, the cavity length of the Fabry-Perot interferometer refers to the distance between the end-face of the microfiber and that of the single-mode fiber, which can be adjusted precisely by 3D fiber adjustments. The microfiber Fabry-Perot interferometer has a microfiber diameter of 73 μm and a cavity length of 39 μm, being experimentally demonstrated with a high-temperature sensitivity of 6.386 nm/°C from 42 °C to 54 °C. An interesting optical modulation phenomenon has also been observed. This compact fiber probe can be used for real-time monitoring of temperature fluctuations in small and complex environments.

1. Introduction

Because of their compact structures and good stabilities, optical fiber interferometers have replaced the traditional interferometers in many applications [1–4]. Compared to Mach-Zehnder, Michelson, and Sagnac fiber interferometers, the Fabry-Perot interferometer has a simpler structure and is easily constructed on a single optical fiber [5]. Additionally, the reflective interference mechanism allows the signal light and reference light to share the same optical fiber, which makes the fiber system highly compact and small volume [6]. In recent years, a variety of fiber Fabry-Perot interferometer structures have fabricated by laser ablation, fiber fusion, magnetron sputtering coating, and polymer flexible film function. The femtosecond laser beam can process air holes through the optical fiber to produce the simple Fabry-Perot interference cavities [7], which can be directly used for detecting gas, liquid and other filling materials' concentration, but is not suitable for mass production due to the high production cost [8]. Furthermore, the phase change in the Fabry-Perot interference is related only to the effective refractive index of the measured medium, resulting in its low sensitivity [9]. In some works, the Fabry-Perot interference cavity was prepared by the cascade-fibers with different structures [10]. The cavity length was controlled by the type and length of the intermediate fusion fiber [11]. These special optical fibers, including the hollow-core optical fibers or photonic crystal optical fibers, usually contain the air holes in which the refractive index or temperature-sensitive gases or liquids were filled to obtain different sensing probes [12–14]. Akin to the above technology, the Fabry-Perot cavity was also prepared from the magnetron sputtering process by coating the fiber end surface with different functional materials having different thicknesses [15]. A resin at the fiber end can be easily cured by UV glue to explore the miniature Fabry-Perot cavities using for sensing the temperature and strain with the high sensing performance [16]. But these fabrication processes are complex and extremely costly. The most cost-effective and simple Fabry-Perot fiber structures were realized by either constructing an

* Corresponding author at: College of Information Science and Engineering, Northeastern University, Shenyang 110819, China.
E-mail addresses: lijin@ise.neu.edu.cn (J. Li), 20174113@stu.neu.edu.cn (Y. Zhang).

https://doi.org/10.1016/j.optlastec.2020.106296
Received 8 January 2020; Received in revised form 4 March 2020; Accepted 18 April 2020
Available online 29 April 2020

open cavity at the fiber end by chemically etching, laser machining, or splicing the normal fiber using a hollow fiber or capillary with precisely controlled length [17,18]. The cavities were then sealed by the flexible polymer membranes made by different sensitive materials [19]. These classes of open-cavity structures have been experimentally demonstrated to have high sensitivity but the serious cross-sensitivity [20,21]. In this paper, a synthesis method for a Fabry-Perot interferometer with a stable structure is reported. It was prepared in a quartz capillary by precisely controlling the microfiber diameter and the distance between the optical fibers. A high-performance temperature sensing probe with sensitivity up to 6.386 nm/°C and a good linearity by filling the air cavity with temperature-sensitive polymer sol through thermoplastic fixation process. A similar structure has been reported earlier by strictly aligning microfiber with single-mode fiber [22]. In this work, the noncoaxial structure with good flexibility and production repeatability was proposed and has been experimental verified.

2. Microfiber Fabry-Perot interferometer temperature probe preparation

The proposed Fabry-Perot structure primarily includes a microfiber, a single-mode fiber, a quartz capillary, and polydimethylsiloxane (PDMS) sol, as shown in Fig. 1(a). The microfiber was made by a multi-functional fiber taper machine (IPCS-5000-ST, Idealphotonics Inc.) using high-temperature flame scanning-stretching technique. Its diameter was fine-tuned by controlling the composition of oxy-hydrogen flame, as well as the scanning speed, the heating time and the stretching speed. The microfiber was cut by a ceramic knife at the desired region under a homemade micromanipulation platform. In addition to the cutting region (also known as microfiber diameter), the surface quality must be tested to eliminate the possible drawbacks. The impact of the end-face quality of microfiber can be found in Fig. 1(b) (D = 60, S = 61). This outcome may be attributed to the tiny defects on the end-face of the microfiber, which leads to the appearance of individual modes of interference (red frame identification) and disturbs the quality of the interference spectrum. A common single-mode fiber with a flat end-face was prepared by peeling off the coated layer. The tail ends of the above two optical fibers were fixed on the high-precision 3D adjustment (APFP-XYZ, adjusting precision < 2 μm, Zolix Instruments Co., LTD), through which the optical fibers were continuously moved inside the capillary to precisely regulate the distance between the two optical fiber ends, and the resulting structure was also monitored under the microscope in real-time. Due to the precise controlling system, the microfiber Fabry-Perot interferometer structure can be produced with the good repeatability and high quality for their reflection spectra.

Fig. 1(b) compares the Fabry-Perot interference spectra for the structures having microfiber diameters of 28 μm, 45 μm, 60 μm, 78 μm and the corresponding cavity lengths of 165 μm, 56 μm, 61 μm, 68 μm and 36 μm, respectively. The free spectrum ranges (FSRs) are 12, 16.5, 17, 19 and 20.5 nm, respectively. The changing trend does not conform to the traditional Fabry-Perot interference principle, wherein the interference phase

$$\Delta\phi = 2(\Delta n_e S)\cdot\frac{2\pi}{\lambda} \tag{1}$$

where Δn_e refers to the effective refractive index of the medium present in the cavity. Along with the cavity length S, we can contribute that the interference phase also depends on the microfiber diameter D with a function of $f(D)$, that is

$$\Delta\phi = 2(\Delta n_e S)\cdot\frac{2\pi}{\lambda} + f(D) \tag{2}$$

Here, $f(D)$ mainly depends on the evanescent field effect on the surface of microfiber. Its strength is exponentially attenuated away from the fiber tip. There are many modes are excited to form the evanescent field, and possessed the different phase changes. The exact form of $f(D)$ cannot be determined precisely. Generally, the optical characteristics of fiber structures with different parameters were obtained by recording and analyzing the changes in intensity and phase for the optical superimposition field. In order to improve its temperature-response sensitivity, and fix the structures, the PDMS gel (basic component: curing agent = 10:1) was prepared and filled into the quartz capillary with a syringe. Both ends of the capillary were sealed with AB

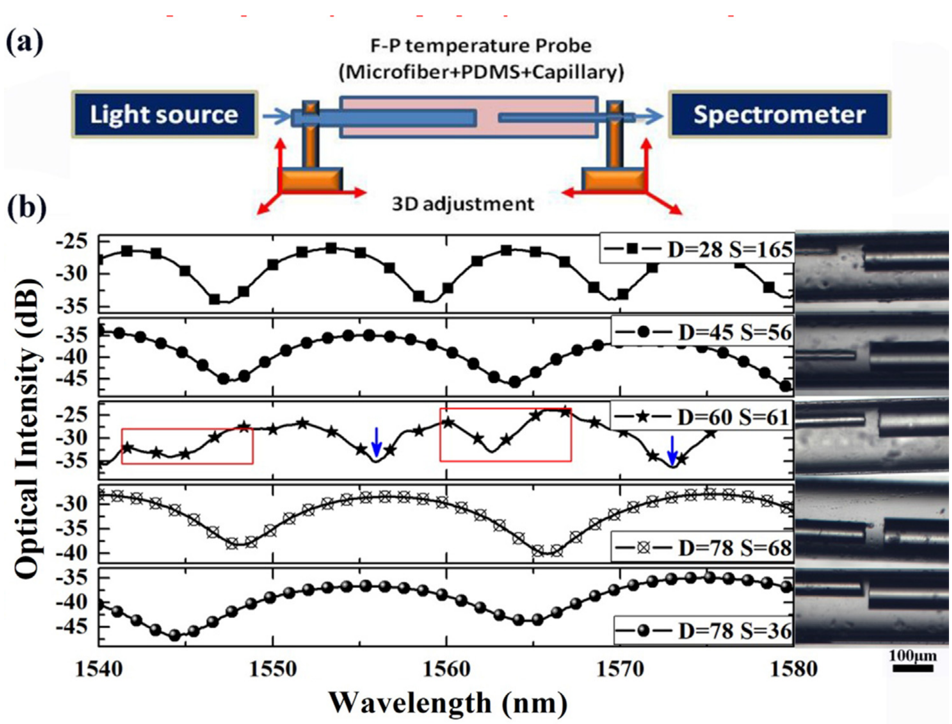

Fig. 1. Experimental schematic for the fabrication and spectra measurement of the microfiber Fabry-Perot interferometer temperature probe (a); the interference spectra and the corresponding microscopic images of the structures with different cavity lengths and microfiber diameters (b).

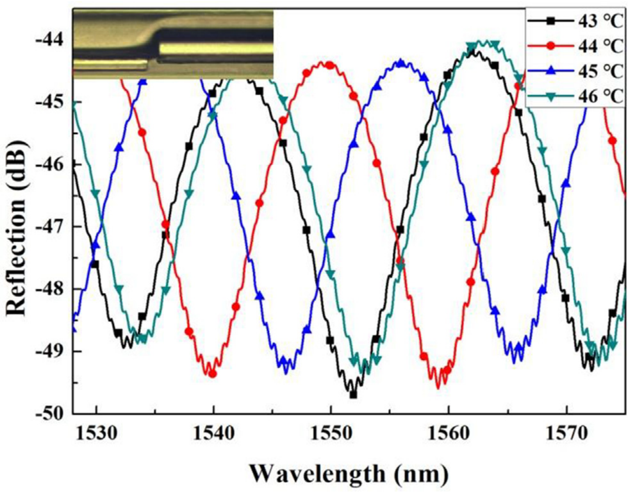

Fig. 2. Reflected spectrum changes as a function of temperature increasing from 43 °C to 46 °C for PDMS-encapsulated microfiber Fabry-Perot temperature probe with non-coaxial alignment, microfiber diameter of 73 μm and cavity length of 39 μm. Inset: Photo of the temperature probe.

glue. The PDMS solution was then placed in a constant-temperature oven to cure at 80 °C for 1 h.

3. Temperature sensing experiment and results analysis

To verify the sensing performance of the as-prepared microfiber Fabry-Perot interferometer, the corresponding temperature calibration system was built. The microfiber Fabry-Perot interferometer temperature probe and thermocouple were placed in a blower type thermostat (Boxun BGZ-30, temperature: 25 °C to 250 °C). Amplified spontaneous emission (ASE) light source (Golight 1550 nm ASE, wavelength: 1520–1610 nm) and optical spectrometer (Yokogawa AQ6370, resolution: 20 pm) were used to supply the incident light and collect the reflected spectra of the Fabry-Perot interferometer at varying temperatures. This temperature-probe had the microfiber diameter and the cavity length of 73 μm and 39 μm, respectively, as well as the axial dislocation of ∼60 μm between the two fibers (as shown in the inset of Fig. 2). In Fig. 1, the two fibers were inserted into the capillary and removed flexibly and continually to study the impact of the microfiber diameter and surface quality on the optical response of Fabry-Perot structures. Here in Fig. 2, a Fabry-Perot interferometer temperature probe with fixed structure parameters was introduced. The two fibers were fixed in the capillary to obtain a cured Fabry-Perot structure using the thermal-solidified PDMS. As illustrated in Fig. 2, the interference spectra red-shifted as the temperature increased from 43 °C to 46 °C.

Wavelength demodulation technology is frequently used for processing the signal of the optical fiber sensor. One needs to record and analyze the wavelength location of the special peak (dip) to obtain the characteristic sensing curve. As a result, the FSR of the interference spectrum strictly limits the working range of the sensor. It is very difficult to distinguish the special peaks (dips) near two different FSRs. In Fig. 2, two special dips can be seen overlapped in the interference spectrum at 46 °C (green color and inverted triangle symbol) and 43 °C (black color and cube symbol). It indicates that the dynamic temperature monitoring range is < 3 °C, and it is problematic to distinguish the different special dips of these two groups of interference spectra beyond this range. Hence, the sensor probe with a small FSR is suitable only for the high-precision monitoring of the temperature fluctuation during a limited range instead of a wide temperature variation. Yet, because the nature of temperature variation is usually continuous in most cases, it is possible to obtain a larger working range by dynamically tracking the position of the special peak (dip).

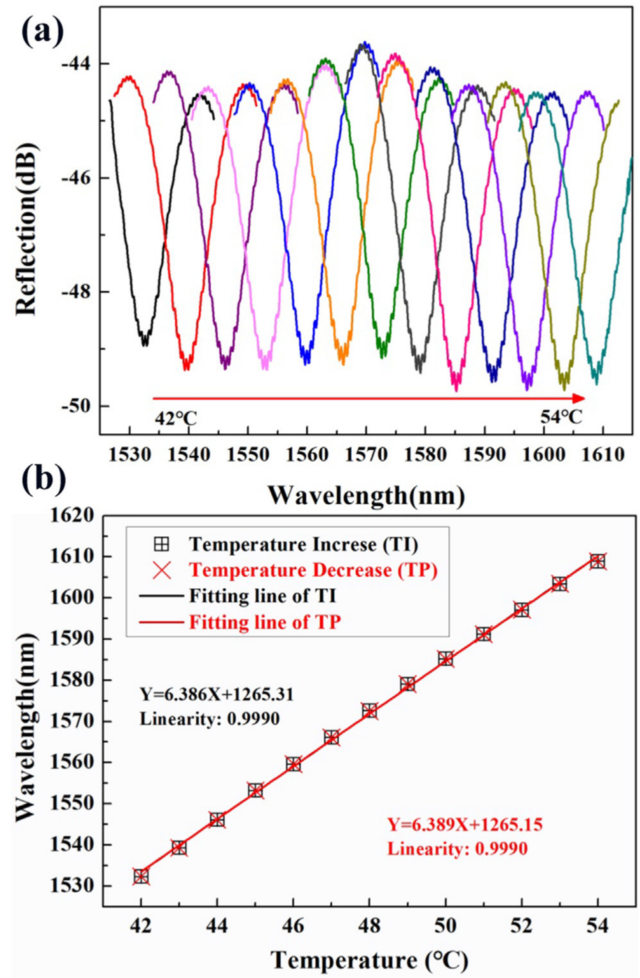

Fig. 3. (a) Reflected spectrum changes as a function of temperature increasing from 42 °C to 54 °C and (b) corresponding temperature-sensing characteristics curve for temperature increasing and decreasing process.

In this experiment, the thermostat has the linear increasing process above 40 °C. The working range of the proposed Fabry-Perot interferometer temperature probe depends on the nature property of the filled PDMS. Although it has the stable physicochemical property during −55 °C to 200 °C, the linear temperature sensing characteristics are obtained only from room temperature (25 °C) to 110 °C in the following experiment. It is impossible to demonstrate its lower sensing performance under room temperature due to the blower type thermostat. Here, a special peak (dip) position was continuously tracked to calibrate the sensing characteristics curve when the temperature was raised from 42 °C to 54 °C with a step interval of 1 °C. If the temperature become higher than 54 °C, the dip will move out the wavelength range of the light source ($>$ 1610 nm). In this stage, one can find another special peak (dip) near 1520 nm to verify its temperature response at higher temperature, as the work reported earlier [22].

To clearly compare the wavelength location of the special peak (dip) in the whole spectrum range, the individual effective spectra were intercepted and compared in Fig. 3(a), in which, the special peak (dip) continuously red-shifted from ∼1533 nm to ∼1609 nm. The temperature sensing characteristics curve was plotted by recording and analyzing the corresponding wavelengths of the initial and the remaining 12 experimental points during the temperature increasing, as shown in Fig. 3(b). The fitting curve of the experimental data for either temperature increase or decrease process shows excellent linearity. Moreover, the wavelength location expresses a uniform moving speed which resulted in an average sensitivity of 6.386 nm/°C from 42 °C to 54 °C,

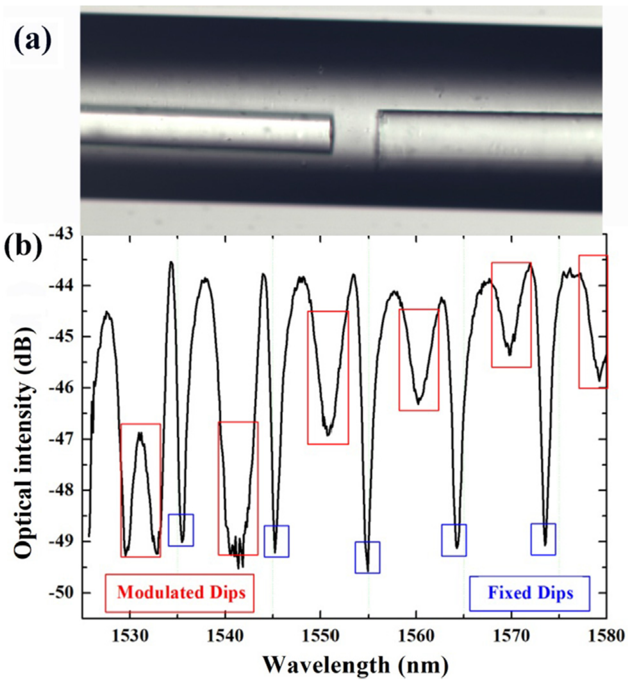

Fig. 4. Microscopic image (a) and optical modulation spectrum of PDMS-encapsulated microfiber Fabry-Perot structure (b).

and an average sensitivity of 6.389 nm/°C from 54 °C to 42 °C. The deviation distribution of 12 experimental data ranges from 0.0012 nm to 0.0041 nm by comparing the different processes of temperature reduction and temperature rise at the same temperature point. Because the resolution of the spectrometer used in this work is 0.02 nm, the corresponding resolution of the proposed temperature probe is calculated to be ~0.003 °C. This result is in the same order of magnitude as a previously published work [23]. The system reveals a high-temperature sensing performance of the microfiber Fabry-Perot interferometer even when the axes of the microfiber and single-mode fiber undergo the significant dislocations.

Moreover, the Fabry-Perot interference spectrum strongly depends on the diameter and the end-face morphology of the microfiber. The influence of microfiber on the interference spectrum is distinctly visible. Fig. 4 shows the special reflection spectrum of the microfiber Fabry-Perot temperature probe. The reflection spectrum contains a series of fixed peaks (dips) at a constant FSR, which are labeled by blue boxes; and another group of modulation dips with a constant FSR and the periodic intensity changes, are labeled by red boxes. The Fabry-Perot interference dips periodically turn out with the quality (Q) factor of ~1261 and FSR of ~9.29 nm. The optical modulation spectrum maybe related with the muti-modes interference effect and evanescent field effect, which come from either the specific micro-structure of the end surface of microfiber or the specific angle between the microfiber tip and single mode fiber. Furthermore, only uniform sine waveform was observed in the reflect spectra of the Fabry-Perot interferometers in Fig. 1. But in this Fabry-Perot interferometer, the diameter of the microfiber tip is ~78 μm, and both microfiber and single mode fiber were fixed by the PDMS. The effect from either diameters or environment fluctuation can be ignored. The intensity changing dips can be used to mark the fixed resonance peak and expand the working range of Fabry-Perot structural fiber sensors.

The sensing performance of the proposed microfiber Fabry-Perot temperature probe was compared with the recently proposed Fabry-Perot structural temperature fiber sensors, as shown in Table 1.

As reviewed in the introduction section, femtosecond laser can be used to machine the air cavity on or through a SMF to explore the fiber sensor working at a high temperature but with a low sensitivity. A splicer can be used to join different fibers together and construct a Fabry-Perot structure usually using hollow core fiber (HCF) or photonics crystal fiber (PCF) with the air holes, in which the liquid will be filled in to optimize their sensing performance.

4. Conclusions

The Fabry-Perot interference structure based on the non-axial microfiber and a single-mode fiber has been fabricated. Its interference spectrum is not only related to the cavity length of the Fabry-Perot structure but also depends strongly on the diameter and surface quality of the microfiber. A variety of higher-order optical modes are excited at the end-face of the microfiber, which may affect the quality of the interference spectrum. It can also produce periodically modulated optical signals, which may be used as reference signals for the Fabry-Perot interference spectrum and be conducive to signal-demodulation or multi-parameter sensing. The relative positions of the microfiber and the single-mode fiber were solidified and encapsulated in a quartz capillary by PDMS sol. The corresponding microfiber diameter and cavity lengths were 73 μm and 39 μm, respectively. The compact microfiber Fabry-Perot temperature probe experimentally demonstrated with a high sensitivity of 6.386 nm/°C and an excellent linearity of 0.9990. This compact micron-level temperature probe is well suited for high sensitivity and environmental stability, which is expected to be used for the high-precision detection for the temperature fluctuations in biological and chemical reactions.

CRediT authorship contribution statement

Jin Li: Funding acquisition, Project administration, Supervision, Writing - review & editing. **Zhoubing Li:** Data curation, Formal analysis, Writing - review & editing. **Juntong Yang:** Writing - original draft. **Yue Zhang:** Investigation, Methodology. **Chunqiao Ren:** Writing - original draft.

Declaration of Competing Interest

The authors declare that they have no known competing financial

Table 1
Sensing performance comparison of proposed sensor with related works.

Structure, Materials and Technology	Production and Cost	Temperature Range (°C)	Sensitivity	Reference
SMF/Vernier effect	Femtosecond laser machine/High	25–1000	927 pm/°C	[7]
SMF		100–500	13.9 pm/°C	[8]
		500–1000	18.6 pm/°C	
SMF/Capillary	Cascaded splicing fiber/Low	100–800	14 pm/°C	[10]
Four-hole fiber/SMF		15–40	−0.115 rad/°C	[20]
SMFs/UV clue	UV-curable resins/Low	25–45	0.48 nm/°C	[16]
HCF/PCF	Splicing fiber/High	25–70	10.64 pm/°C	[21]
Photonic bandgap fiber	Liquid filling/Low	25–55	−1.94 dB/°C	[24]
Microfiber/PDMS	Solid package/Low	25–110	6.386 nm/°C	This work

interests or personal relationships that could have appeared to influence the work reported in this paper.

Acknowledgement

This work was supported by the National Key R&D Program of China (2019YFB2006001), Fundamental Research Funds for the Central Universities, China (N2004007), and Joint Research Fund Liaoning-Shenyang National Laboratory for Materials Science, China (20180510015).

Appendix A. Supplementary data

Supplementary data to this article can be found online at https://doi.org/10.1016/j.optlastec.2020.106296.

References

[1] D. Inaudi, A. Rüfenacht, B. Von Arx, H.P. Noher, S. Vurpillot, B. Glisic, Monitoring of a concrete arch bridge during construction, Smart Structures and Materials 2002: Smart Systems for Bridges, Structures, and Highways, Int. Soc. Opt. Photo. 4696 (2002) 146–153.
[2] B. Glisic, D. Inaudi, Integration of long-gage fiber-optic sensor into a fiber-reinforced composite sensing tape, Smart Structures and Materials 2003: Smart Sensor Technology and Measurement Systems, Int. Soc. Opt. Photo. 5050 (2003) 179–186.
[3] É. Pinet, C. Hamel, B. Glisic, D. Inaudi, N. Miron, Health monitoring with optical fiber sensors: From human body to civil structures, Health Monitoring of Structural and Biological Systems 2007, Int. Soc. Opt. Photo. 6532 (2007) 653219.
[4] X.Y. Sun, D.K. Chu, X.R. Dong, H.T. Li Chu-Zhou, Y.W. Luo-Zhi, J.Y. Zhou Hu, J.A. Duan Cong-Wang, Highly sensitive refractive index fiber inline Mach-Zehnder interferometer fabricated by femtosecond laser micromachining and chemical etching, Opt Laser Technol 77 (2016) 11–15.
[5] A.G. Leal-Junior, L.M. Avellar, C.A. Díaz, A. Frizera, C. Marques, M.J. Pontes, Fabry-Perot curvature sensor with cavities based on UV-curable resins: Design, Analysis and Data fusion approach, IEEE Sensors J. 19 (21) (2019) 9798–9805.
[6] B. Du, X.Z. Xu, J. He, K.K. Guo, W. Huang, F.C. Zhang, M. Zhang, Y.P. Wang, In-fiber collimator-based Fabry-Perot interferometer with enhanced vibration sensitivity, Sensors-Basel 19 (2) (2019) 435.
[7] T. Paixao, F. Araujo, P. Antunes, Highly sensitive fiber optic temperature and strain sensor based on an intrinsic Fabry-Perot interferometer fabricated by a femtosecond laser, Opt. Lett. 44 (19) (2019) 4833–4836.
[8] P.C. Chen, X.W. Shu, Refractive-index-modified-dot Fabry-Perot fiber probe fabricated by femtosecond laser for high-temperature sensing, Opt. Express 26 (5) (2018) 5292–5299.
[9] P.F. Liu, L. Jiang, S.M. Wang, Z.T. Cao, P. Wang, Temperature-insensitive refractive index sensor based on an optical fiber extrinsic Fabry-Perot interferometer processed by a femtosecond laser, Chin. Opt. Lett. 14 (2) (2016) 020602.
[10] Y.F. Wu, Y.D. Zhang, J. Wu, P. Yuan, Simultaneous measurement of transverse load and temperature using hybrid structured fiber-optic Fabry-Perot interferometer, Sci. Rep.-Uk 7 (2017) 10736.
[11] K. Ott, S. Garcia, R. Kohlhaas, K. Schuppert, P. Rosenbusch, R. Long, J. Reichel, Millimeter-long fiber Fabry-Perot cavities, Opt. Express 24 (9) (2016) 9839–9853.
[12] L. Yan, Z.G. Gui, G.J. Wang, Y.Q. An, J.Y. Gu, M.Q. Zhang, X.L. Liu, Z.B. Wang, G. Wang, P.G. Jia, A micro bubble structure based Fabry-Perot optical fiber strain sensor with high sensitivity and low-cost characteristics, Sensors-Basel 17 (3) (2017) 555.
[13] Y. Zhao, M.Q. Chen, R.Q. Lv, F. Xia, In-fiber rectangular air Fabry-Perot strain sensor based on high-precision fiber cutting platform, Opt. Commun. 384 (2017) 107–110.
[14] C.B. Zhang, T.G. Ning, J.J. Zheng, J. Xu, X.K. Gao, H. Lin, J. Li, L. Pei, An optical fiber strain sensor by using of taper based TCF structure, Opt. Laser Technol. 120 (2019).
[15] N.P. Poluektov, Y.P. Tsar'gorodsev, I.I. Usatov, A.G. Evstigneev, Energy flux to the substrate in a magnetron discharge with hollow cathode, Thin Solid Films 640 (2017) 60–66.
[16] A.G. Leal-Junior, C.R. Díaz, C. Marques, A. Frizera, M.J. Pontes, Analysis of viscoelastic properties influence on strain and temperature responses of Fabry-Perot cavities based on UV-curable resins, Opt. Laser Technol. 120 (2019) 105743.
[17] M.F. Domingues, C.A. Rodriguez, J. Martins, C. Tavares, C. Marques, N. Alberto, P. Andre, P. Antunes, Cost-effective optical fiber pressure sensor based on intrinsic Fabry-Perot interferometric micro-cavities, Opt. Fiber Technol. 42 (2018) 56–62.
[18] H. Liao, P. Lu, L. Liu, S. Wang, W.J. Ni, X. Fu, D.M. Liu, J.S. Zhang, Phase demodulation of short-cavity Fabry-Perot interferometric acoustic sensors with two wavelengths, IEEE Photo. J. 9 (2) (2017) 1–9.
[19] W.P. Chen, D.N. Wang, B. Xu, C.L. Zhao, H.F. Chen, Multimode fiber tip Fabry-Perot cavity for highly sensitive pressure measurement, Sci. Rep.-Uk 7 (2017) 368.
[20] C.L. Wang, G.F. Yan, Z.G. Lian, X. Chen, S.N. Wu, S.L. He, Hybrid-cavity Fabry-Perot interferometer for multi-point relative humidity and temperature sensing, Sensor Actuat. B-Chem. 255 (2018) 1937–1944.
[21] Y.D. He, H.Z. Yang, K.S. Lim, H. Ahmad, Z.Y. Feng, P. Zhang, Q. Tian, K. Lu, Z. Han, J. Liu, Discriminative measurement for temperature and humidity using hollow-core Fabry-Perot interferometer, Opt. Fiber Technol. 53 (2019) 102027.
[22] J. Li, Q. Nie, L.T. Gai, H.Y. Li, H.F. Hu, Highly sensitive temperature sensing probe based on deviation S-shaped microfiber, J. Lightwave Technol. 35 (17) (2017) 3706–3711.
[23] Z.B. Li, Y. Zhang, C.Q. Ren, Z.Q. Sui, J. Li, A high sensitivity temperature sensing probe based on microfiber Fabry-Perot interference, Sensors-Basel 19 (8) (2019) 1819.
[24] T. Han, Y.G. Liu, Z. Wang, Z. Wu, S. Wang, S. Li, Simultaneous temperature and force measurement using Fabry-Perot interferometer and bandgap effect of a fluid-filled photonic crystal fiber, Opt. Express 20 (12) (2012) 13320–13325.